08

Fabrication, study of normal metal-insulator-superconductor junctions Al/AlO$_x$/Nb

© M.A. Markina,[1,2] A.M. Chekushkin,[1] M.A. Tarasov,[1] M.Yu. Fominskiy,[1] T.D. Patsaev,[3] A.L. Vasiliev[3]

[1]Kotelnikov Institute of Radio Engineering and Electronics, Russian Academy of Sciences,
125009 Moscow, Russia
[2]National Research University Higher School of Economics,
109028 Moscow, Russia
[3]Shubnikov Institute of Crystallography RAS,
59119333 Moscow, Russia
e-mail: markina_ma@hitech.cplire.ru

Received May 15, 2024
Revised May 15, 2024
Accepted May 15, 2024

The paper presents the design, fabrication and research of structures based on normal metal-insulator-superconductor tunnelling junctions. The morphology of the three-layer Al/AlO$_x$/Nb structure has been analyzed by transmission electron microscopy, transmission scanning electron microscopy and electron diffraction methods. Selective Niobium Etching and Anodization Process technology was used to form tunnel junctions. The fabricated devices, in which the role of superconductor is performed by Nb, are able to work as thermometers in the temperature range of 1.5-8 K. The quality parameter of the fabricated structures was achieved - the ratio $R_d/R_n(V=0)=53$ at a temperature of 2.8 K, while the theoretically expected value is 54. The design of structures of series and parallel connected tunnel elements has been developed, the peculiarity of such a design is that the area of the normal metal is large, which means that its electronic system will be reliably thermalised, so such a design will be preferable for thermometry. Integrated thermometer structures whose dR/dT is larger than that of a single tunnelling junction have been fabricated. Normal metal-insulator-superconductor structures based on niobium can be used as thermometers, detectors as well as electronic coolers.

Keywords: tunnel junction, normal metal-insulator-superconductor (NIS), chains of NIS contacts, SNEAP (Selective Niobium Etching and Anodization Process), plasma-chemical etching, transmission electron microscopy (TEM).

DOI: 10.61011/TP.2024.07.58804.169-24

Introduction

Normal metal-insulator-superconductor junction (NIS junction) detectors have been widely recognized as high-sensitive receiving devices in a wide frequency band from 0.1 to 1 THz [1–3]. The main material used in such structures is Al that has a superconducting transition temperature of 1.2 K, and operating temperatures of these detectors are 0.3 K and lower. The paper describes the development, fabrication and study of Nb and Al NIS junctions at boiling points of liquid helium (4.2 K): niobium ($T_c = 9.2$ K) goes into the superconducting state, and Al ($T_c = 1.2$ K) remains in the normal metal state. Increase in operating temperature of NIS junction structures makes it possible to avoid bulky and sophisticated dilution cryostats.

Classical method used to produce NIS junctions is a shadow sputtering method [4], however, the properties of thermally deposited niobium are worse than that in magnetron sputtering [5]. The study optimizes the deposition process of Al/AlO$_x$/Nb sandwich structure, which is produced without vacuum break using magnetron sputtering followed by fabrication of NIS junctions by the contact photolithography method.

When measuring the response of the receiving structure to radiation, it is important to know not only the temperature of absorber, but also to understand whether the electronic temperature of the receiving structure has been increased initially due to thermal noise or electric interference. The paper describes the development and fabrication of NIS junction chains that may function as a thermometer placed immediately on the test sample.

1. Operating principle

At a temperature below T_c, Nb goes to the superconducting state, the current-voltage curve (CVC) of the Al/AlO$_x$/Nb normal metal-insulator-superconductor junction becomes nonlinear. When a voltage lower than the bandgap width is applied, current flowing through the junction grows exponentially, and when higher voltages are applied, current tends to asymptotic value of V/Rn. At $T \ll T_c$, $\Delta(T)$, where Δ is the energy bandgap in the superconductor energy spectrum, T is the electronic system temperature, becomes constant and approaches $\Delta(0)$. Full tunnel current through the superconductor-insulator-normal metal junctions is defined by the difference of $I_{S\to N}$ and

$I_{S\to N}$ of tunneling electrons. In case of low voltages on the junction and when $T \ll T_c$ and $U < \Delta/e$ are satisfied, the shape of NIS junction CVC may be described with high accuracy using expression [2,6,7]:

$$I = \frac{1}{eR_n}\sqrt{2\pi kT\Delta}\exp\left(\frac{-\Delta}{kT}\right)\sin h\left(\frac{eV}{kT}\right), \qquad (1)$$

where V is voltage applied to the NIS junction, e is the electron charge, k is the Boltzmann constant.

Therefore, the single-particle tunneling current at the applied voltages $U < \Delta/e$ will depend on the asymptotic resistance of the junction and normal metal electron temperature. Using the tunnel junction CVC measurements, we can estimate the electronic temperature of metal using equation (1), therefore the structure based on NIS junctions may be used for thermometry without additional calibration.

Thermometers consisting normal metal-insulator-superconductor (NIS) junctions connected in parallel and in series were designed. The samples consist of cells and each cell contains 8 NIS junctions connected by the bottom electrode. NIS components formed on different cells are interconnected by the top superconducting Nb electrode forming the multielement structures (Figure 1). The design features formation of a normal large-area electrode used to reliably thermalize the electronic systems of the normal electrode. The study investigates structures consisting from 40, 80 or 200 NIS junctions connected in series and in parallel. Figure 2 shows the photograph of a structure consisting of 40 NIS components. Such structure will ensure increase in reliability of the structure, because if one of the junctions fails (as a result of absence of stripping by the lift-off lithography method in case of small-area junctions or loss of contact between near-by NIX junctions, etc.), this will affect the operating parameters (R_n and, consequently, also R_d will be changed), but the structure will still function properly — current will flow through other connections in the chain. Connection of NIS junctions into series/parallel chains gives a higher asymptotic resistance and, accordingly, higher differential resistance of the sample resulting in an increase of the response dR/dT of the structure by a factor of 2.5, 5 and 12.5, respectively.

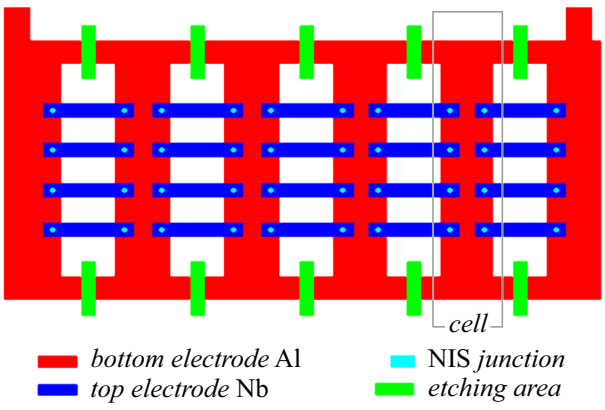

Figure 1. Diagram of a thermometer consisting of 40 NIS junctions.

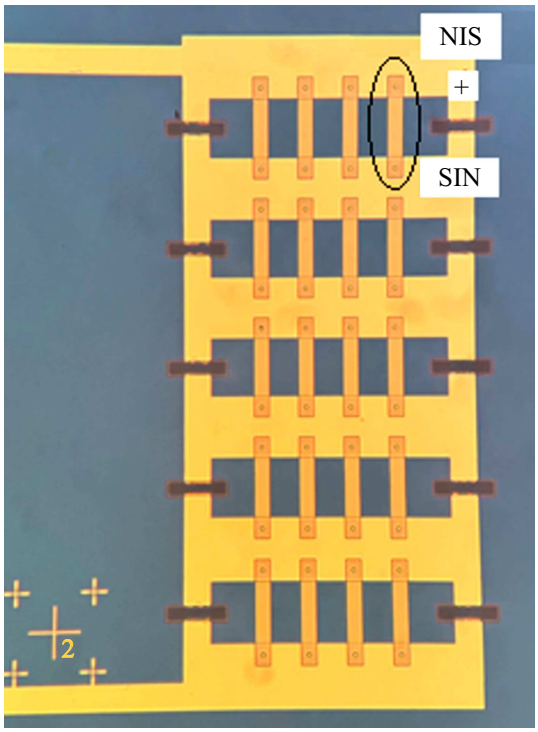

Figure 2. Photograph of a structure consisting of 40 NIS junctions.

2. Target parameters

As a result of current differentiation (1) with respect to voltage provided that the abovementioned conditions are met, an expression for differential conductance will be derived. Differential resistance is a reciprocal quantity

$$R_d = \frac{dV}{dI} = R_n\sqrt{\frac{kT}{2\pi\Delta}}\exp\left(\frac{\Delta}{kT}\right)\left\{\cos h\left(\frac{eV}{kT}\right)\right\}^{-1}, \qquad (2)$$

where R_n is the asymptotic resistance of the tunnel junction at applied voltages much higher than V_g.

If both sides of (2) are divided by R_n, then in the right-hand side an expression will be obtained value of which at the given voltage V depends only on the electron temperature in the normal metal layer. For a single structure at 4.2 K, the theoretically expected value is $R_d/R_n = 9.68$. However, this ratio may be lower due to thermal noise and electric interference effects or shunting of the measured structures caused by micro short circuits on the fabricated junctions. Value of this parameters is used to judge whether there are any micro short circuits or thermal and electric interference.

In series and parallel connection of structures, R_d/R_n for the junction chain remains the same as for a single NIS junction, therefore the quality of the multielement structure may be also estimated by the value of this parameter. The

maximum nonlinearity voltage equation (2) will vary as a multiple of the number of junctions connected in series in the structure.

To assess the tunnel barrier quality, we use R_nS, where S is the area of the fabricated junction. The test substrates were used to form the junctions with various diameters, therefore R_n for them will be different, and R_nS for an ideally made tunnel barrier shall be identical. R_nS spread on the test substrate may be used to estimate the degree of uniformity of the grown insulator layer and, consequently, whether the employed technique is applicable to fabrication of multicomponent structures. When significant deviations of R_nS from the mean value on the substrate are observed for a particular junction, then nonuniformity of the tunnel barrier in the junction area is suggested.

3. Description of the fabrication technique

Shadow thermal bias Al sputtering method is the classical method of NIS-junction fabrication. However, the thermally deposited Nb is worse in terms of its properties than that obtained by the magnetron sputtering method, therefore we investigate the fabrication process of the Al/AlO_x/Nb sandwich structure without vacuum break using magnetron sputtering followed by fabrication of NIS-junction by the SNEAP technique.

To protect the substrate against corrosion at the following plasma-enhanced chemical etching stages, 100 nm of Al_2O_3 is deposited on the Si substrate using the magnetron high-frequency (HF) sputtering method. Then, a photoresist mask is formed on the substrate by the photolithography method to define the geometry of the base electrode, then a sandwich structure is made within one vacuum cycle. The 100 nm bottom Al layer is deposited by DC magnetron sputtering in argon plasma. The barrier layer is formed by thermal oxidizing of the Al surface in pure oxygen at a constant pressure of 10 mbar and room temperature (20 °C). Oxidizing time varied, barrier transparency and, consequently, R_nS depend on the oxidizing time (Table 1). After Al oxidizing, a 80–100 nm top Nb layer is applied by the magnetron sputtering method.. Section 4 shows the images of the Al/AlO_x/Nb normal metal-insulator-superconductor structure made using the transmission electron microscopy.

The NIS junction area is formed by the SNEAP method using plasma-enhanced chemical etching in chemically active CF_4 plasma by removing the top Nb layer of the multilayer structure on the photoresist mask (contact photolithography). In CF_4 plasma, the AlO_x layer is not etched and serves as a stop layer preventing further etching of the structure. Then, anodization in ethyleneglycol ammonia pentaborate solution is performed, as a result an oxide layer grows on the perimeter of the NIS junction to avoid possible micro short circuits on the junction ends. Then the RF-magnetron sputtering method is used to apply a 250 nm SiO_2 layer to ensure insulation between the base and top feed electrodes. Contacts to the junctions are opened by the lift-off lithography method. The top Nb electrode and Al or Au contact pads are also made by the lift-off contact photolithography and argon-plasma DC sputtering.

Table 1. Oxidation parameters

Thermal oxidizing time, min	R_nS of sample, $k\Omega \cdot \mu m^2$
30	2.25 ± 0.09
10	0.92 ± 0.03

Junction chains are made using the same technique: a sandwich structure is made initially, then NIS junctions are formed. To perform the anodization of the multicomponent structure, all junctions are fabricated on a common electrode and, thus, they have a common electric contact in the bottom base electrode layer. After sputtering of a contactor and contact pads, the sandwich structure is etched through to remove the anodization bridges (Figure 1). Note that when sputtering the SiO_2 insulation layer, the anodization bridge areas are closed by the resist in order to perform the etching process later in these places. The sandwich structure is etched through in two stages: etching of the top Nb layer during 65 s in chemically active CF_4 plasma, then chemical etching of AlO_x and Al in 1% KOH water solution during 80 s. The whole product, except the areas where the sandwich structure is to be removed, is coated by the resist to protect it against plasma-enhanced chemical and liquid etching. Note that resist thickness reduction is observed, but about 1 μm of resist is left after both etching stages and this is sufficient to prevent etching of the whole structure.

4. Cross-sectional analysis of the Al-AlO_x–Nb sandwich structure

Morphology of the sandwich structure and crystallographic properties of the deposited materials have been examined using the transmission electron microscopy (TEM), transmission scanning-electron microscopy (TSEM) and electron diffraction (ED). For study by the TEM/TSEM/ED methods, a cross cut of the structure was made by the focused ion beam method in Versa double-beam ion-electron microscope (Thermofisher Scientific, USA). A Pt layer was deposited on the sample surface. The analysis was performed using Osiris transmission/scanning electron microscope (T/SEM) (ThermoFisher Scientific, USA) with an accelerating voltage of 200 kV with a dark-field detector (Fischione, USA) and SuperX energy-dispersive spectrometer (Bruker, USA).

The sample was deposited onto a Si(001) substrate. The brightfield TEM image of the Al/AlO_x/Nb sandwich structure cut is shown in Figure 3, *a*. Figure 3, *b* shows the cuts of the whole test structure: Si substrate, Al_2O_3

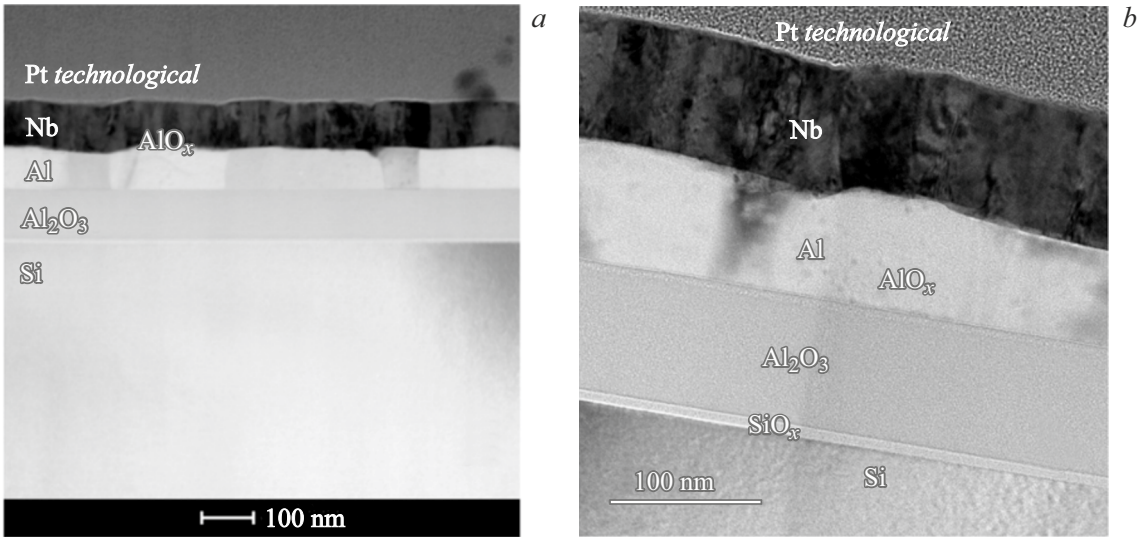

Figure 3. brightfield image of Al/AlO$_x$/Nb in TEM.

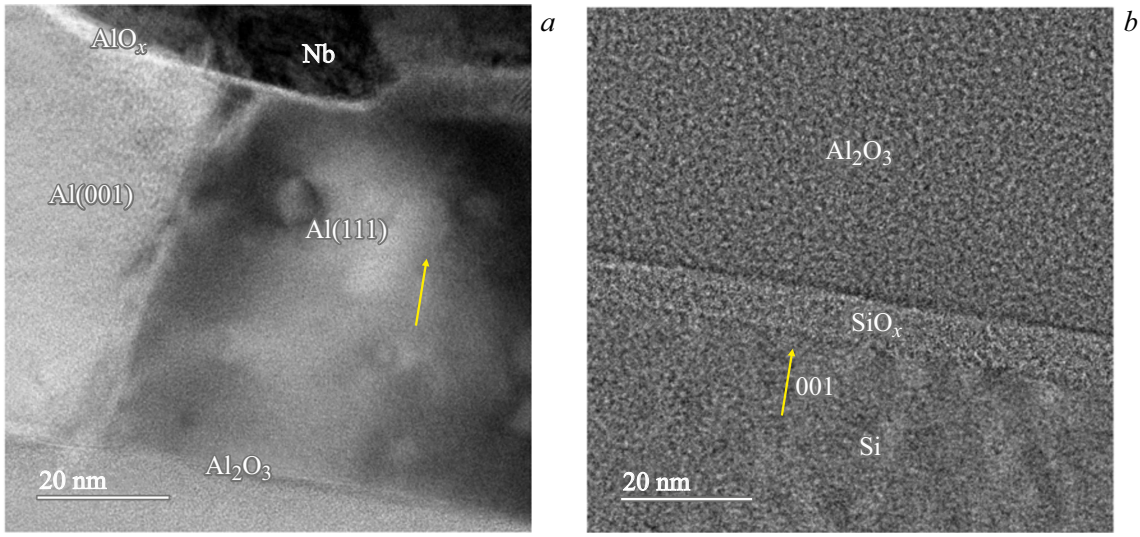

Figure 4. Electron-beam images of Al/AlO$_x$/Nb.

stop layer, Al/AlO$_x$/Nb structure of interest, there is also a process platinum layer necessary for proper structural examination by the TEM, TSEM and ED methods.

It can be seen that film growth with Nb and Al crystallites takes place during magnetron sputtering and the bottom electrode film contains irregularities. Since the next layers duplicate the bottom Al surface, irregularities are still present in the Al/AlO$_x$/Nb that is fabricated later. Paper [8] reports that the tunnel barrier in the irregularity areas will be the most transparent and this means that the tunnel current will flow mainly through them. If the fabricated NIS junction falls into the area of such irregularity, then its quality and main properties will be probably degraded.

The electron-beam image (Figure 4, *a*) shows a Al$_2$O$_3$ layer, then — the sandwich structure of interest: Al layer where regions with various Al orientation are present, thin AlO$_x$ tunnel barrier and top Nb electrode. Figure 4, *b* shows the Si(001) substrate orientation, natural oxide layer on the substrate and Al$_2$O$_3$ stop layer deposited on the substrate. The TEM analysis suggests that substrate and deposited Al orientations are different, and also regions with different Al orientation occur. This may affect the quality of the fabricated tunnel junctions.

5. CVC analysis of the samples

Test samples of single tunnel junctions and structures with NIS chains connected in parallel and series were fabricated using the described technique. The samples were measured in liquid helium at $T = 4.2$ K. The samples were also examined in Gifford-McMahon closed-loop cryostat

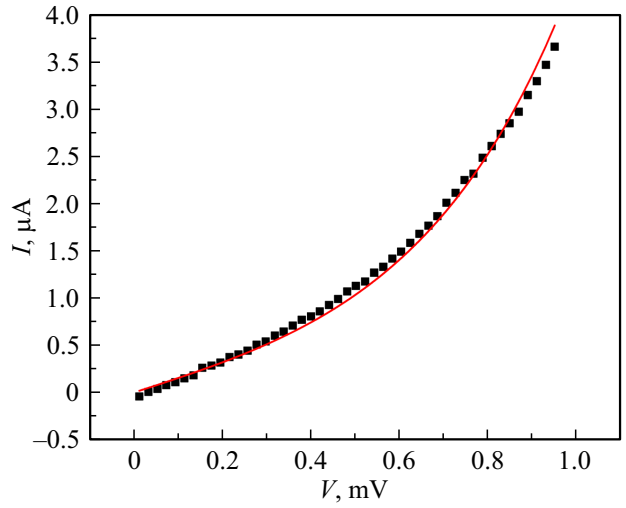

Figure 5. CVC of NIS single junction (boxes) and its approximation by the theoretical curve (solid line) at $T = 4.2$ K.

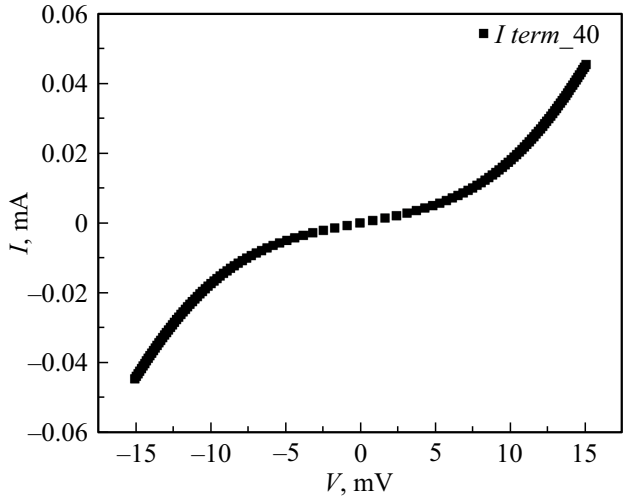

Figure 6. CVC of a structure consisting of 40 NIS junctions.

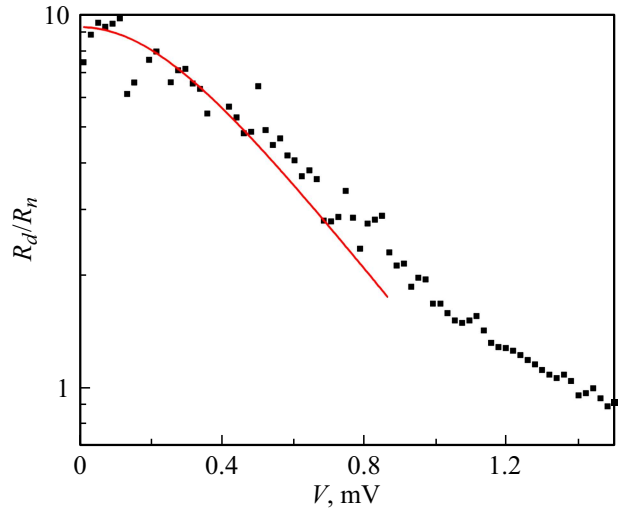

Figure 7. R_d/R_n of NIS junction of test_11 sample. Boxes — experiment, solid curve — approximation. $(R_d/R_n)_{\max} = 9.23$.

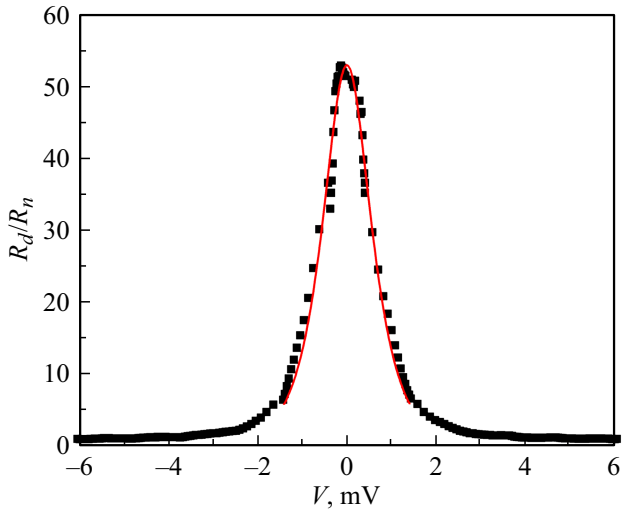

Figure 8. R_d/R_n of NIS junction of test_21 sample at 2.8 K. Boxes — experiment, solid curve — approximation. (R_d/R_n) max $= 53.0$.

with an operating temperature of 2.8 K. CVC of the structurers were recorded in the four-point pattern.

CVC of a single NIS structure in liquid-helium measurement (junction area $\sim 15\,\mu\text{m}^2$) and its approximation by theoretical equation (1) for single current are shown in Figure 5. Nb bandgap in superconducting state $\Delta \approx 1.35 - 1.4$ meV. Figure 6 shows CVC of the structure consisting of 20 NIS components, total bandgap $\Delta \approx 14$ meV is observed, which meets the design because 10 NIS junctions are connected in series.

Figure 7 shows the experimental dependence R_d/R_n on bias voltage and theoretical curve approximation. Theoretically expected R_d/R_n at 4.2 K is 9.68. The maximum observed on test structures at zero voltage $R_d/R_n = 9.23$. We believe that the difference of the observed typical parameter is attributed to the presence of micro short circuits on the perimeter of NIS junction and also by electric interference due to insufficient screening and filtration, which is associated with the features of the measuring system.

Figure 8 shows the dependence of R_d/R_n on the supplied voltage at 2.8 K on the test structure and its theoretical curve approximation. Experimental parameter has its maximum value $R_d/R_n = 53.00$. The calculation according to equation (2) results in the maximum theoretical value $R_d/R_n(V = 0) = 54.58$ at 2.8 K.

Figure 9 shows dependences of the differential resistance $R(V)$ of chains consisting of 40, 80 and 200 NIS junctions. As shown in the figure, it can be suggested that the response to the supplied voltage variation with respect to the resistance of the structure consisting of more

Table 2. Main properties of single and multicomponent NIS structures

Sample	d of a single junction, μm	R_nS, $\Omega \cdot \mu m^2$	Number of junctions connected in series	R_d/R_n	$T_{measured}$, K
test_21	5.42 ± 0.10	1036.3	2	53.00	2.8
test_11	4.38 ± 0.03	903.3	1	9.23	4.2
test_11	3.35 ± 0.03	901.4	1	8.35	4.2
Term ch1	9.74 ± 0.03	921.4	10	8.33	4.2
			20	8.60	4.2
Term ch2	3.83 ± 0.03	934.3	10	7.33	4.2
			20	7.56	4.2
Term ch3	5.76 ± 0.03	932.8	10	8.51	4.2
			20	8.97	4.2
			50	9.25	4.2

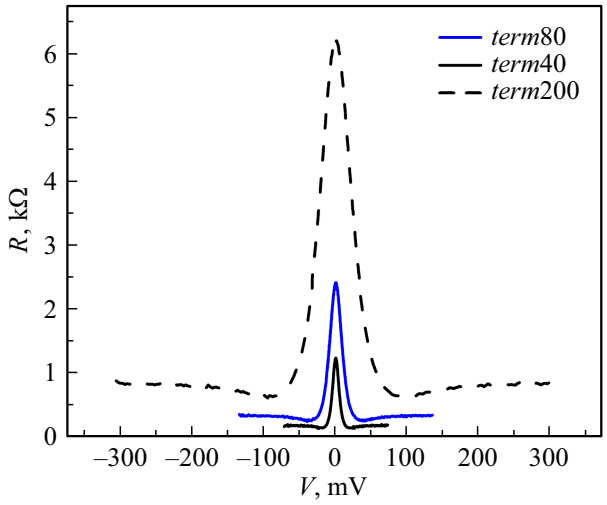

Figure 9. $R(V)$ at $T = 4.2$ K for NIS junction chains.

components is higher than that of a single junction, i.e. $dR_{50}/dV > dR_{10}/dV$.

Table 2 shows values of R_nS and R_d/R_n for single and multicomponent structures at different temperatures.

Mean value of R_n=0.92±0.03 kΩ·μm^2 at an oxidizing time of 10 min; R_n=2.25±0.09 kΩ·μm^2 at an oxidizing time of 30 min. Maximum rms deviation R_nS on the 24×24 mm substrate does not exceed 8%, i.e. the barrier layer fabrication method ensures uniform oxide thickness and repeatability of the barrier transparency.

The mean value of R_d/R_n observed on single test structures corresponds to 8.79 ± 0.47. The maximum deviation R_d/R_n from the mean value on the 24×24 mm substrate does not exceed 4%. R_d/R_n for different multicomponent structures is shown in Table 2. The data show that R_d/R_n increases with the number of junctions for various thermometers. We suppose that the thermal noise (Nyquist noise) of the measuring unit facilitates the parameter degradation, and the single NIS is subjected to various interference and noise, and in case of chains, high series resistance reduces the current from EDS interference and thermal noise, thus, reducing the current smear. The measured R_d/R_n of large structures is higher because their noise-to-current ratio is lower than dI/I of the structure with lower number of components. In [9], to reduce thermal interference, the operating structure was measured according to the four-point pattern through 4 additional NIS junctions that played the role of a ballast resistance that had the same temperature as the test structure. Such „cold“ resistors induced less thermal noise in measurements than the resistors having room temperature in the measurement circuit. To check our assumption, we are planning to conduct measurements with cold resistors. For this, a resistance element may be added to the structure by modifying the design. If the structures are measured in the cooling cryostat, then the ballast resistance may be placed directly on the cooling stage in the unit.

Conclusion

A NIS structure fabrication technique using magnetron sputtering and junction area formation by the SNEAP method is proposed. Samples with Nb and Al NIS junctions were made. A quality parameter for the fabricated structures was achieved: for $T = 2.8$ K, $R_d/R_n = 53.00$ with theoretically expected 54.58. The tested technique is used to make high quality NIS junctions and may be used, for example, to create receiving structures, coolers and thermometers.

Using the Al/AlO$_x$/Nb NIS junctions, structures suitable for thermometry were made. Measurements of long NIS junction chains compared with the structures consisting of less components and single NIS have shown higher values

of R_d/R_n close to theoretically expected values. Since the estimated parameter spread of test single junctions made on the same substrate has shown that the quality of junctions is the same throughout the substrate, we believe that most junctions constituting the NIS arrays have good similar quality and the obtained results show that there are problems associated with the presence of interference and thermal loads in CVC measurements. To control thermal noise during CVC measurements, measurements with cold resist are planned. Measurements of response with respect to resistance to temperature variation in multicomponent structures, comparison of temperature sensitivity of samples with different number of junctions are also planned.

Paper [10] shows that the optimization of the growth of bottom Al layer results in the improvement of uniformity of the formed barrier thickness and, consequently, to the optimization of properties of the whole test structure. Therefore, to improve the quality of the bottom electrode and to verify the effect of this factor on the quality of the fabricated junction, $Al/AlO_x/Nb$ structures are to be fabricated in future by sputtering onto a hot (up to 400 °C) or cold (77 K) substrate, and morphology of the produced crystals as well as orientation of film growth on a substrate with other Si(111) orientation preferable for Al(111) film growth are to be investigated.

Acknowledgments

Equipment of Unique Research Unit № 352529 „Kriointegral“ was used for sample fabrication.

Funding

Test sample fabrication and experimental measurements were supported by grant of RSF №23-79-10262 (https://rscf.ru/project/23-79-10262/). Examination of the morphology of the fabricated structures was supported by the project of the Ministry of Science and Higher Education (Agreement № 075-15-2024-538).

Conflict of interest

The authors declare that they have no conflict of interest

References

[1] J. Clarke, G.I. Hoffer, P.L. Richards. Rev. Phys. Appliqué, **9** (1), 69 (1974). DOI: 10.1051/rphysap:019740090106900
[2] D. Golubev, L. Kuzmin. J. Appl. Phys., **89** (11), 6464 (2001). DOI: 10.1063/1.1351002
[3] M. Tarasov, L. Kuz'min, E. Stepantsov, I. Agulo, A. Kalabukhov, M. Fominskii, Z. Ivanov, T. Claeson. J. Experim. Theor. Phys. Lett., **79** (6), 298 (2004). DOI: 10.1134/1.1759413
[4] J. Niemeyer. PTB-Mitt, **84** (4), 251 (1974).
[5] F.M. Al-Ghamdi, A. Ennawy, R.J. Bennett, A. Vradis. J. King Abdulaziz University-Science, **5** (1), 99 (1993). DOI: 10.4197/Sci.5-1.9
[6] I. Giaever. Phys. Rev. Lett., **5** (10), 464(1960). DOI: 10.1103/PhysRevLett.5.464
[7] I. Giaever, K. Megerle. Phys. Rev., **122** (4), 1101(1961). DOI: 10.1103/PhysRev.122.1101
[8] L.J. Zeng, S. Nik, T. Greibe, P. Krantz, C.M. Wilson, P. Delsing, E. Olsson. J. Phys. D: Appl. Phys., **48** (39), 395308 (2015). DOI: 10.1088/0022-3727/48/39/395308
[9] S. Fritz, L. Radtke, R. Schneider, M. Weides, D. Gerthsen. J. Appl. Phys., **125** (16), 165301 (2019). DOI: 10.1063/1.5089871
[10] A. Vystavkin, D. Shuvaev, L. Kuzmin, M. Tarasov, E. Adersted, M. Villander, T. Klaeson. ZhETF, **115** (3), 1085 (1999). (in Russian).

Translated by E.Ilinskaya